Synthesis, Crystal and Magnetic Structure of the Double Perovskites A_2NiMoO_6 (A = Sr, Ba): A Neutron Diffraction Study

María J. Martínez-Lope,[a] José A. Alonso,*[a] and María T. Casais[a]

Keywords: Perovskites / Neutron diffraction / Magnetic properties / Nickel

A_2NiMoO_6 (A = Sr, Ba) perovskites have been prepared in polycrystalline form by thermal treatment, in air, of previously decomposed citrate precursors. These materials have been studied by X-ray (XRD) and neutron powder diffraction (NPD) data. At room temperature, the crystal structure is tetragonal, space group $I4/m$, for Sr_2NiMoO_6 and for Ba_2NiMoO_6 the crystal structure is cubic, space group $Fm\bar{3}m$. Both perovskites contain divalent Ni cations. The low temperature antiferromagnetic ordering has been followed from sequential neutron diffraction data. Peaks of magnetic origin appear in the NPD patterns below temperatures of T_N = 81.2 K and T_N = 64.3 K for the Sr and Ba compounds, respectively. The magnetic structures are defined by a propagation vector $\mathbf{k}$ = (1/2,0,1/2) for Sr_2NiMoO_6 and $\mathbf{k}$ = (1/2,1/2,1/2) for Ba_2NiMoO_6. The refined magnitude of the Ni magnetic moments also suggests a divalent oxidation state with $S = 1$.

Introduction

The double-perovskite oxides of general formula $A_2B'B''O_6$, in which A is a rare-earth metal and B′ and B′′ are transition metal cations, constitute a wide family of materials displaying varied and appealing electronic and magnetic properties. More than 300 compounds with the double-perovskite structure have been synthesized so far,[1] in which the perovskite B sites are occupied alternately by different cations B′ and B′′. These materials have recently attracted the interest of materials scientists for possible applications in magnetoresistive devices, since the report of room temperature colossal magnetoresistance (CMR) in the double perovskite Sr_2FeMoO_6.[2] Similar CMR properties have also been described in other complex perovskites, such as Sr_2ReMoO_6 and Ba_2FeMoO_6,[3−8] for which the CMR effect seems to be due to intergrain tunneling.[8,9]

The ideal structure of these compounds can be viewed as a regular arrangement of corner-sharing $B'O_6$ and $B''O_6$ octahedra, alternating along the three directions of the crystal, with the voluminous A cations occupying the voids between the octahedra. When the size of the A cations decreases with respect to that of B′ and B′′ cations, there is a reduction in symmetry from cubic to tetragonal or even monoclinic due to the tilting of the $B'O_6$ and $B''O_6$ octahedra. For instance, Ba_2FeMoO_6 is cubic over the temperature range 2−300 K, whereas Sr_2FeMoO_6 is cubic above the ferromagnetic Curie temperature, and undergoes a structural phase-transition and becomes tetragonal ($I4/m$) below this temperature.[10−12] Sr_2CoMoO_6 is tetragonal[13] and the crystal contains alternating CoO_6 and MoO_6 octahedra, moderately tilted by 6.7° in the basal *ab* plane. Ca_2FeMoO_6 is monoclinic,[14] with a significant tilt of the FeO_6 and MoO_6 octahedra, due to the small size of the Ca cations found at the A positions.

The Ni analogues of A_2FeMoO_6 (A = Sr, Ba) have attracted our attention. The double perovskites Sr_2NiMoO_6 and Ba_2NiMoO_6 were studied in the sixties and then forgotten for more than 30 years. Sr_2NiMoO_6 was described as tetragonal,[15−17] and an antiferromagnetic behaviour has been observed below T_N = 80 K (17). Ba_2NiMoO_6 was described as cubic with a = 4.02 Å.[15−16]

In the present work we describe the synthesis of A_2NiMoO_6 (A = Sr, Ba), prepared by soft chemistry procedures, and the results of a neutron powder diffraction (NPD) study on well-crystallized samples. The crystal structures have been revised and we report complete structural data for these perovskites. Low-temperature NPD data allowed us to probe the microscopic origin of the antiferromagnetic ordering, and the evolution of the ordered Ni^{2+} magnetic moment.

Results

The double perovskites A_2NiMoO_6 (A = Sr, Ba) were obtained as nicely crystalline powders, the XRD diagrams for which are shown in Figure 1. The diffraction pattern for the Ba compound is characteristic of a cubic perovskite structure, showing superstructure peaks corresponding to the Ni/Mo ordering. The Sr_2NiMoO_6 XRD diagram shows the splitting of certain reflections, characteristic of a tetragonal distortion [for instance the (004) and (220) reflections].

[a] Instituto de Ciencia de Materiales de Madrid, CSIC, Cantoblanco, 28049 Madrid, Spain

 DOI: 10.1002/ejic.200300063

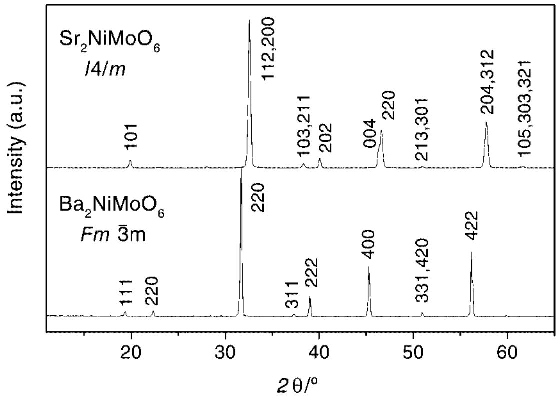

Figure 1. XRD patterns for A_2NiMoO_6 (A = Sr, Ba), indexed in a tetragonal unit cell with $a = b = \sqrt{2}a_0$, $c = 2a_0$ (A = Sr) and $a = 2a_0$, **(**A = Ba**)**, $a_0 \approx 4$ Å

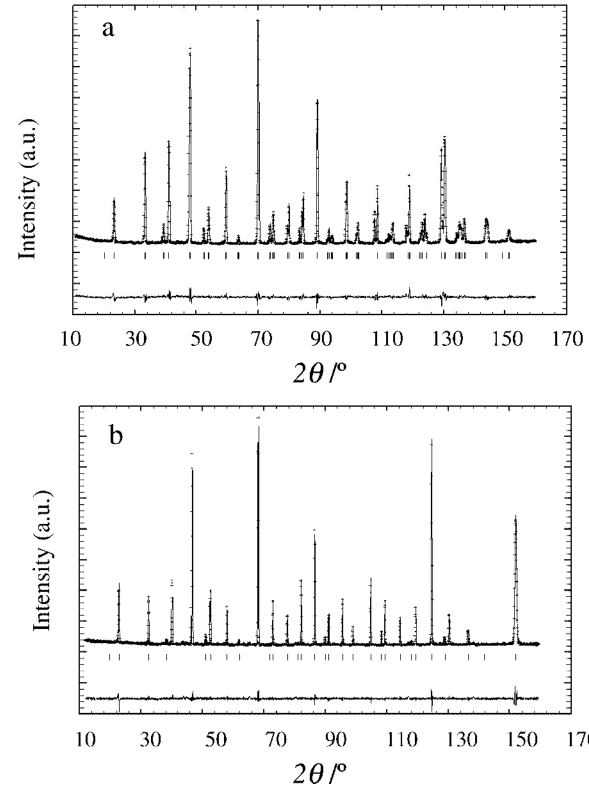

Figure 2. Observed (crosses), calculated (full line) and difference (bottom) high resolution NPD Rietveld profiles for A_2NiMoO_6 collected at 295 K with λ = 1.594 Å for (a) A = Sr, (b) A = Ba

Structural Refinement

For Sr_2NiMoO_6, the structural refinement from room temperature high resolution NPD data was performed in the $I4/m$ space group (no. 87), $Z = 2$, with unit-cell parameters related to $\mathbf{a_o}$ (ideal cubic perovskite: $\mathbf{a_o}$ = 3.9 Å) as $\mathbf{a} = \mathbf{b} = \sqrt{2}\mathbf{a_o}$, $\mathbf{c} = 2\mathbf{a_o}$. The Sr atoms were located at 4d positions, Ni at 2a, Mo at 2b sites, and oxygen atoms at 4e and 8 h positions. For Ba_2NiMoO_6, the structural refinement from room temperature high-resolution NPD data was performed in the $Fm\bar{3}m$ space group (no. 225), $Z = 4$, with unit-cell parameters related to $\mathbf{a_o}$ (ideal cubic perovskite, $\mathbf{a_o}$= 3.9 Å) as $\mathbf{a} = \mathbf{b} = \mathbf{c} = 2\mathbf{a_o}$. The Ba atoms are located at the 8c positions, Ni at 4a, Mo at 4b sites, and oxygen atoms at the 24e positions. An excellent fit was obtained for these models, as shown in Figure 2. In the final refinement, the possibility of anti-site disordering was checked by assuming that some Ni atoms could occupy Mo sites, and vice-versa: the refinement of the inversion degree led to less than 1% of anti-site disordering. The oxygen stoichiometry was also checked by refining the occupancy factors of the oxygen atoms; no deficiency was detected within the standard deviations. The most important structural parameters of the crystallographic structure at room temp. and the discrepancy factors after the refinements are listed in Table 1. The main interatomic distances and angles are included in Table 2. A view of the crystal structures is shown in Figure 3.

The tetragonal unit-cell of Sr_2NiMoO_6 is smaller than the cubic one of Ba_2NiMoO_6, normalizing per formula unit, as expected for the smaller ionic radius of Sr^{2+} (1.26 Å) versus Ba^{2+} (1.42 Å) in 12-fold coordination.[19] It is interesting to note the significant expansion of the Ni−O interatomic distances (Table 2) from the Sr compound [Ni−O: 2.024(4) Å] to the Ba perovskite [Ni−O: 2.097(2)] upon scaling the larger size of the unit cell for the Ba compound.

Magnetic Structure

The magnetic structure for A_2NiMoO_6 (A = Sr, Ba) and its thermal evolution was analyzed from a set of NPD patterns collected in the temperature range 2< T <87 K, with λ = 2.42 Å. In Sr_2NiMoO_6, on cooling to below 81.2 K, new reflections appear at positions forbidden for the Bragg reflections in the space group $I4/m$. These new peaks arise from the establishment of a long-range magnetic ordering defined by a propagation vector $\mathbf{k}$ = (1/2, 0, 1/2). An antiferromagnetic structure was modeled with magnetic moments at the Ni positions; after the full refinement of the profile, including the magnetic moment magnitude, a best discrepancy factor of R_{mag} = 12.6% was reached for the 2 K diagram considering the Ni moment to be approximately aligned along the [101] direction. In Ba_2NiMoO_6 the new peaks appear below T_N = 64.3 K and are indexed in the cubic cell with the propagation vector $\mathbf{k}$ = (1/2, 1/2, 1/2). The determination of the orientation of the moments is not possible in a cubic structure from powder data, therefore in the refinement we supposed that the moments lie along the [0 0 1] direction. After the refinement of the antiferromagnetic structure, a discrepancy factor of R_{mag} = 14.0% was obtained for the 2 K diagram. The goodness of both fits at 2 K is illustrated in Figures 4a and 4b.

The magnetic structure of the two compounds is stable from 2 K to T_N, as demonstrated in a sequential refinement of all the available temperature range. The thermal evolution of the Ni magnetic moments is illustrated in Fig-

Table 1. Positional and thermal parameters for A_2NiMoO_6 (A= Sr, Ba), from NPD data at 295 K; the unit cell parameters for A = Sr (*I*4/*m* space group) are $a = b = 5.54939(5)$ Å, $c = 7.89554(9)$ Å, $V = 243.149(4)$ Å^3; for A = Ba ($Fm\bar{3}m$ space group) they are $a = b = c = 8.04862(3)$ Å, $V = 521.392(4)$ Å^3

Atoms	Positions	A = Sr	A = Ba
A	x	0.00	0.25
	y	0.50	0.25
	z	0.25	0.25
	B(Å^2)	0.70(2)	0.33(2)
Ni	x	0.00	0.00
	y	0.00	0.00
	z	0.50	0.00
	B(Å^2)	0.19(5)	0.26(5)
Mo	x	0.00	0.50
	y	0.00	0.00
	z	0.00	0.00
	B(Å^2)	0.56(9)	0.34(8)
O1	x	0.00	0.2605(3)
	y	0.00	0.00
	z	0.2426(6)	0.00
	B(Å^2)	0.86(4)	0.46(2)
O2	x	0.2689(4)	
	y	0.2187(5)	
	z	0.00	
	B(Å^2)	0.86(3)	
	R_p	4.38%	5.03%
	R_{wp}	5.83%	6.60%
	R_{exp}	3.47%	5.10%
	χ^2	2.83	1.68
	R_I	3.55%	2.11%

Table 2. Main bond lengths (Å) and selected angles (°) for tetragonal Sr_2NiMoO_6 and cubic Ba_2NiMoO_6 determined from NPD data at 295 K

	A = Sr	A = Ba
A−O1	(× 4) 2.7753(1)	(× 12) 2.8469(1)
A−O2	(× 4) 2.926(2)	
A−O2	(× 4) 2.648(2)	
<A−O>	2.783(1)	2.8469(1)
Ni−O1	(× 2) 2.032(5)	(× 6) 2.097(2)
Ni−O2	(× 4) 2.020(3)	
<Ni−O>	2.024(4)	2.097(2)
Mo−O1	(× 2) 1.916(5)	(× 6) 1.927(2)
Mo−O2	(× 4) 1.924(3)	
<Mo−O>	1.921(4)	1.927(2)
Ni−O1−Mo	180.0	180.0
Ni−O2−Mo	168.5(1)	

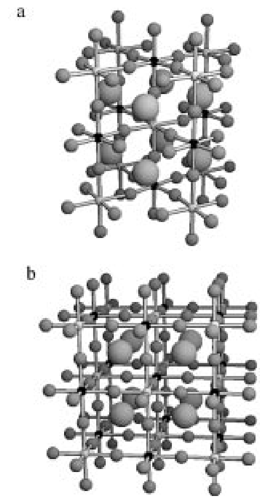

Figure 3. Two views of the crystal structure of the A_2NiMoO_6 double perovskites for (a) A = Sr, (b) A = Ba; within the octahedra, Ni atoms (small dark spheres) alternate with Mo atoms (small light spheres) in such a way that each NiO_6 octahedron is linked to six MoO_6 octahedra.

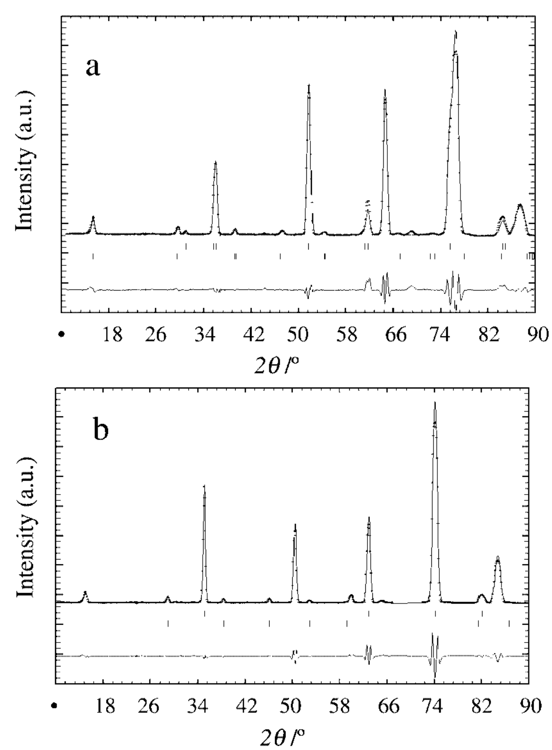

Figure 4. Observed (solid circles), calculated (solid line) and difference (bottom line) NPD patterns collected at 2 K with $\lambda = 2.42$ Å; the two series of tick marks correspond to the crystallographic and magnetic Bragg reflections: (a) Sr_2NiMoO_6 (b) Ba_2NiMoO_6

ures 5a and 5b. The ordered magnetic moments obtained at 2 K are 1.92(6) μ_B and 2.04(6) μ_B for A = Sr and A = Ba, respectively. A view of the magnetic structure of both materials is displayed in Figures 6a and 6b. In both cases, the magnetic arrangement can be described as a stacking of ferromagnetic layers of Ni moments, coupled antiferromagnetically.

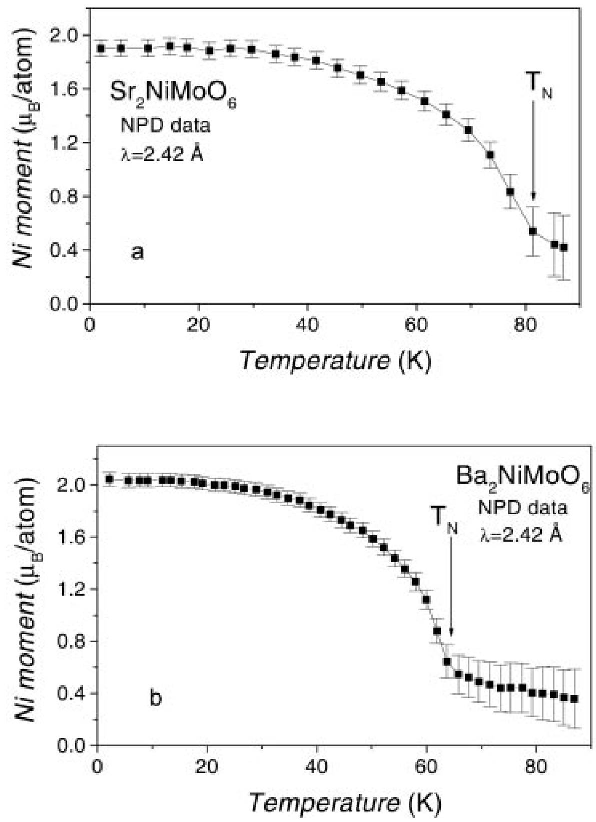

Figure 5. Thermal variation of the ordered magnetic moments for Ni in the antiferromagnetic structure of A_2NiMoO_6: (a) A = Sr (b) A = Ba

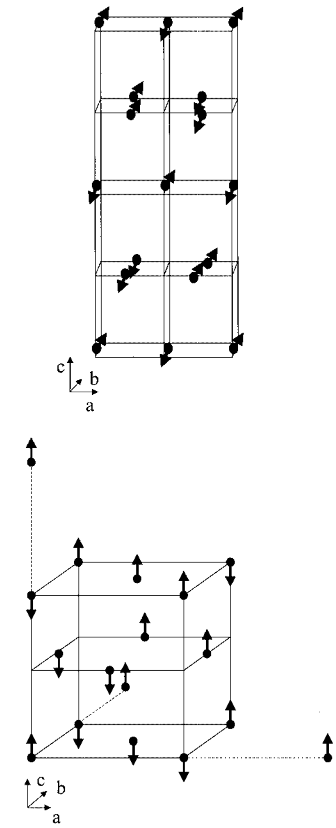

Figure 6. A sketch of the magnetic structures for: (a) Sr_2NiMoO_6, with k = (1/2 0 1/2); the magnetic unit cell consists of four crystallographic cells, and (b) Ba_2NiMoO_6, with k = (1/2 1/2 1/2); for the sake of clarity, the figure shows the chemical cell ($a \approx 8$ Å) and part of three adjacent cells

Discussion

The Ba compound adopts the well-known $(NH_4)_3FeF_6$ structure, which has been described for a large number of complex perovskites showing 1:1 long range order at the B sublattice. In this cubic structure, the BO_6 octahedra are not tilted, with B−O−B angles of 180°. The reduction of ionic size from Ba to Sr implies a reduction in symmetry from cubic to tetragonal, due to the tilting of the NiO_6 and MoO_6 octahedra along the c axis. According to Glazer's nomenclature,[20] the observed tilting is described as $a^0a^0c^-$, implying an antiphase tilting (from layer to layer) along c. The space group $I4/m$ is the one deduced by Woodward[21] for 1:1 double perovskites for the $a^0a^0c^-$ system. The magnitude of the tilting can simply be derived from the Ni−O−Mo angle (φ), as (180 − φ)/2 = 5.75°.

In both perovskites, NiO_6 and MoO_6 octahedra are almost fully ordered and alternate along the three directions of the crystal in such a way that each NiO_6 octahedron is linked to six MoO_6 octahedra, and vice versa. Figure 3 illustrates this particular feature nicely. The driving force for the Ni/Mo ordering is the charge difference between both kinds of cations, since the size difference is not too large. As shown in Table 2, the NiO_6 octahedra are only slightly larger (expanded) than the MoO_6 octahedra in both perovskites. This observation is consistent with the larger ionic size of Ni^{2+} vs. Mo^{6+}. The average Ni−O bond lengths at room temperature compare well with the expected values calculated as the sum of the ionic radii:[19] for A = Sr, <Ni−O> = 2.024(4) Å (calcd. 2.090 Å); <Mo−O> = 1.921 (4) Å (calcd. 1.99 Å); for A = Ba, <Ni−O> = 2.097(2) Å (calcd. 2.090 Å); <Mo−O> = 1.927 (2) Å (calcd. 1.99 Å).

A bond-valence calculation[22,23] from the observed bond lengths can give some insight into the actual oxidation states of the different cations present in the crystal structure. In Sr_2NiMoO_6, the calculated valences for Sr, Ni and Mo are 2.08, 2.21 and 5.78, respectively; in Ba_2NiMoO_6, the calculated valences for Ba, Ni and Mo are 2.66, 1.81 and 5.70, respectively. These values suggest an electronic configuration for these compounds at 298 K given by $Ni^{2+}(3d^8)$ − $Mo^{6+}(4d^\circ)$. The electronic configuration for Ni^{2+} is in good agreement with the results of the magnetic-structure determination at 2 K. These configurations seem to exclude the presence of a mixed valence at the Ni atoms and imply a hexavalent oxidation state for the Mo cations, accounting for the electrical insulating behavior and colored aspect of these samples. The Ba cation seems to be significantly overbonded, exhibiting a valence much higher than the expected 2+ value. In fact, the observed Ba−O distances are much shorter (2.85 Å, see Table 2) than expected from the sum of the ionic radii (3.01 Å). It seems that the much more covalent network determined by NiO_6 and MoO_6 octahedra mainly determines the size of the unit cell; the low degree of freedom of this cubic structure constrains the Ba−O bond lengths outside of the optimal values. However, in the tetragonal structure of Sr_2NiMoO_6, the observed valence for Sr, very close to 2+, suggests that the tilt of the octahedra effectively relieves the stress at the A positions, thus optimizing the Sr−O distances.

In relation to the ordered magnetic moment obtained for Ni cations from the refinement of the magnetic structure at 2 K, it saturates to values close to 2 μ_B for both the Sr and Ba compounds. Again, this fact suggests a divalent oxidation state for the Ni cations ($t_{2g}^6e_g^2$, $S = 1$). The slightly higher Néel temperature observed for the Sr compound (T_N = 81.2 K) with respect to the Ba perovskite (T_N = 64.3 K) implies the presence of stronger magnetic interactions for the former oxide. These interactions are related to the significantly shorter Ni−O distances observed in Sr_2NiMoO_6, which account for a stronger overlap between the Ni 3d and O 2p orbitals, thus enhancing the superexchange process giving rise to the establishment of the antiferromagnetic ordering. In agreement with this observation, the saturation moment of the Ni^{2+} cations is slightly lower for the Sr compound (see Figure 5), again indicating a stronger covalent contribution to the Ni−O bonding in the Sr material, and a more ionic, weaker Ni−O bond with a larger localized magnetic moment for Ni in Ba_2NiMoO_6.

Conclusions

We have presented a detailed crystallographic study of the double perovskites A_2NiMoO_6 (A = Sr, Ba) from NPD data, allowing us to characterize subtle structural features relating the nature and strength of the Ni−O chemical bonds to the ordered magnetic moments determined by neutron diffraction. These compounds experience a low-temperature, long-range antiferromagnetic ordering, concerning the Ni^{2+} magnetic moments. For Sr_2NiMoO_6 the magnetic structure is defined by **k** = (1/2, 0, 1/2), and for Ba_2NiMoO_6 the magnetic structure is defined by **k** = (1/2, 1/2, 1/2). The slightly lower ordered magnetic moment and the greater Néel temperature observed for the Sr perovskite is related to the shorter, more covalent Ni−O bonds determined for this compound. It seems clear that Ni adopts a divalent oxidation state, and Mo is in an hexavalent $4d^0$ configuration, thus explaining the insulating behavior and the colored nature of these complex oxides.

Experimental Section

A_2NiMoO_6 (A = Sr, Ba) perovskites were prepared as ochre (A = Sr) or yellowish green (A = Ba) polycrystalline powders from citrate precursors obtained by soft chemistry procedures. Stoichiometric amounts of analytical grade $Sr(NO_3)_2$, $Ba(NO_3)_2$, $Ni(NO_3)_2{\cdot}6H_2O$ and $(NH_4)_6Mo_7O_{24}{\cdot}4H_2O$ were dissolved in citric acid. The citrate + nitrate solutions were slowly evaporated, leading to organic resins containing a random distribution of the involved cations at an atomic level. These resins were first dried at 120 °C and then slowly decomposed at temperatures up to 600 °C. All the organic materials and nitrates were eliminated in a subsequent treatment at 800 °C in air, for 2 h. This treatment gave rise to highly reactive precursor materials, which were then treated in air for 12 h at 1000 °C (Sr perovskite) or at 1100 °C (Ba perovskite).

The initial characterization of the products was carried out by laboratory X-ray diffraction (XRD) (Cu-K_α, λ = 1.5406 Å). Neutron powder diffraction (NPD) diagrams were collected at the Institut Laue-Langevin (ILL) in Grenoble (France). The crystallographic structures were refined from the high resolution NPD patterns, acquired at room temperature at the D2B diffractometer with λ = 1.594Å. For the determination of the magnetic structures and the study of their thermal variation, a series of NPD patterns were obtained at the D20 high-flux diffractometer (ILL-Grenoble) with a wavelength of 2.42 Å, in the temperature range from 2 to 87 K for (A = Sr, Ba). The refinements of both crystal and magnetic structures were performed by the Rietveld method, using the FULLPROF refinement program.[24] A pseudo-Voigt function was chosen to generate the line shape of the diffraction peaks. The coherent scattering lengths for Sr, Ba, Ni, Mo and O were 7.02, 5.70, 10.300, 4.86 and 5.803 fm, respectively.

Acknowledgments

We are grateful for financial support from the Spanish Ministry of Science and Technology under the project MAT2001−0539, and we are grateful to ILL for making all its facilities available.

[1] M. T. Anderson, K. B. Green Wood, G. A. Taylor, K. R. Poeppelmeier, *Prog. Solid State Chem.* **1993**, *22*, 197.
[2] K. I. Kobayashi, T. Kimura, H. Sawada, K. Terakura, Y. Tokura, *Nature* **1988**, *395*, 677.
[3] K. I. Kobayashi, T. Kimura, Y. Tomioka, H. Sawada, K. Terakura, Y. Tokura, *Phys. Rev. B* **1999**, *59*, 11159.
[4] B. García-Landa, C. Ritter, M. R. Ibarra, J. Blasco, P. A. Algarabel, R. Mahendiran, J. García, *Solid State Commun.* **1999**, *110*, 435.
[5] D. D. Sarma, E. V. Sampathkumaran, S. Ray, R. Nagarajam, S. Majundar, A. Kumar, G. Malini, T. N. Guru Row, *Solid State Commun.* **2000**, *114*, 465.
[6] J. Gopalakrishnan, A. Chattopadhyay, S. B. Ogale, T. Venkatesan, R. L. Greene, A. J. Millis, K. Ramesha, B. Hannoyer and Marest, *Phys. Rev. B* **2000**, *62*, 9538.
[7] D. Niebieskikwiat, R. D. Sánchez, A. Caneiro, L. Morales, M. Vázquez-Mansilla, F. Rivadulla, L. E. Hueso, *Phys. Rev. B* **2000**, *62*, 7033.
[8] A. Maignan, B. Raveau, C. Martin, M. Hervieu, *J. Solid State Chem.* **1999**, *144*, 224.
[9] H. Y. Huang, S. W. Cheong, N. P. Ong, B. Batlogg, *Phys. Rev. Lett.* **1996**, *77*, 2041.
[10] F. K. Patterson, C. W. Moeller, R. Ward, *Inorg. Chem.* **1963**, *2*, 196.
[11] F. Galasso, F. Douglas, R. J. Kasper, *Chem. Phys.* **1966**, *44*, 1672.
[12] O. Chmaissen, R. Kruk, B. Dabrowski, D. E. Brown, X. Xiong, S. Kolesnik, J. D. Jorgensen, C. W. Kimball, *Phys. Rev. B* **2000**, *6*, 14197.
[13] M. C. Viola, M. J. Martínez-Lope, J. A. Alonso, P. Velasco, J. L. Martínez, J. C. Pedregosa, R. E. Carbonio, M. T. Fernández-Díaz, *Chem. Mater.* **2002**, *14*, 812.
[14] J. A. Alonso, M. T. Casais, M. J. Martínez-Lope, J. L. Martínez, P. Velasco, A. Muñoz, M. T. Fernández-Díaz, *Chem. Mater.* **2000**, *12*, 161.

[15] F. Galasso, Structure, *Properties and Preparation of Perovskite-Type Compounds*, Pergamon Press, Oxford **1969**.
[16] L. Brixner, *J. Phys. Chem.* **1960**, *64*, 165.
[17] M. F. Kupriyanov, E. G. Fesenko, *Soc., Phys. Cryst.* **1962**, *7*, 358.
[18] Landolt-Bornstein, *Zahlenwerte und Funktionen aus Naturwissenschaften und Technik*, Neue Serie, Band 4, Teil A, Springer-Verlag, Berlin **1970**.
[19] R. D. Shannon, *Acta Crystallogr., Sect. A* **1976**, *32*, 751.
[20] A. M. Glazer, *Acta Crystallogr.* Sect. B **1972**, *28*, 3384.
[21] P. M. Woodward, *Acta Crystallogr.* Sect. B **1997**, 5 *3*, 32.
[22] I. D. Brown, *in Structure and Bonding in Crystals* (Eds.: M. O'Keefe, A. Navrotsky) Academic Press, New York **1981**, vol. 2, p.1.
[23] N. E. Brese, M. O'Keefe, *Acta Crystallogr., Sect. B* **1991**, *47*, 192.
[24] J. Rodríguez-Carvajal, *Physica B (Amsterdam)* **1993**, *192*, 55.

Received January 31, 2003

